Scientific Research and Essays Vol. 6(32), pp. 6681-6694, 23 December, 2011
Available online at http://www.academicjournals.org/SRE
DOI: 10.5897/SRE11.1333
ISSN 1992-2248 ©2011 Academic Journals

Full Length Research Paper

Mathematical modeling for analysis cable structures

Hashamdar H[1,2]*, Tahir M[2], Z. Ibrahim[2], Jameel M[2], H.B. Mahmud[2], Jahangirzadeh[2]

[1]Steel Technology Center (STC), University of Technology, Malaysia.
[2]Department of civil Engineering, University of Malaya, Kuala Lumpur, Malaysia.

Accepted 24 August, 2011

The cable structures are long tension structures. The main aim of this paper is to provide a new efficient method in all aspects of analysis of tension structures. Tension structures belong to high-nonlinearity structures. The approach of the proposed method is based on the principle of conservation of energy. In this paper a theory for nonlinear dynamics response analysis of tension structure is based on the minimization of the total potential dynamic work developed.

Key words: Fletcher- Reeves method, optimization of energy, finite element method, perturbation technique, analyzing modal, nonlinear dynamic response.

INTRODUCTION

The non-linear systems have no fixed sets of eigenvectors and eigenvalues. The new sets of eigenvectors and eigenvalues must be calculated at each time step and the stiffness matrix must be revaluated at the end of each time step. This makes the use of conventional methods extensively time consuming and costly. The dynamic response analysis of non-linear system is based on the evaluation of response for a series of short time intervals using different types of time integration techniques (Aschheim et al., 2007). The dynamic problems do not have a single solution like static counterparts. The analyst must establish a succession of solution corresponding to all times of interest in the response period. In the dynamic problems, the differential equations arising from the equilibrium of the dynamic forces acting on the mass is solved by implicit or explicit methods. The implicit or explicit method provides numerical solutions to the equations of motion set up for one interval of time. They assume the structural properties to remain constant during the interval, but revaluate them at the end of time step. This may not be sufficient for highly non-linear structures. It is important to revaluate both the stiffness and damping during the time step. The implicit method offers unconditional stability at the expense of operating with relatively dense decomposed matrices when applied to linear structures, but lose the advantage of unconditional stability when applied to non-linear systems (Buchholdt et al., 1982). The explicit methods, on the other hand, use relatively less computer storage, but are hampered by instability which limits the size of the time steps. The implicit methods when applied to non-linear structures require the solution of a set of non-linear equations whilst most explicit methods require the inversion of a non-diagonal matrix. Hence, it is impossible to choose any of these methods as the best, unless the type of structure to be analyzed is specified. As a final step, reduction of time consumption with costly and high accurate result justifies the use of indirect methods such as optimization theory (Ha, 2005).

The present research is based on application of optimization theory. The optimization theory and techniques is used as a real-valued objective function and decrease time consuming and costly. A new algorithm is proposed which converges more rapidly to the neighborhood of solution. The developed method is found to be suitable technique for minimization of total potential energy function especially in cases where the number of variables is large and the structure is highly nonlinear. The present method decreases computational time and number of iterations required per time step.

The tension structures have many advantages such as prefabrication, ease of transportation and erection, relatively low cost and provision for coverage of large clear spans and high strength, large flexibility and elasticity. The design process is a relatively complex problem. In the present study we consider the effect of dynamic loads in tension structures and describe a

*Corresponding author. E-mail: hashamdar@gmail.com.

Fletcher-Reeves method for the determination of free and forced vibration analysis of structures. The Fletcher-Reeves method belongs to a group of methods which attempt to locate a local minimum function. Fletcher-Reeves algorithm is applied to calculate the set of displacements that to minimize the energy of structural system (Hashamdar et al., 2011a; Kukreti, 1989).

The minimization of the total potential dynamic work is indirect method which based on principle of convergence of energy in structures. Conventional methods such as superposition methods are direct method. They are usually employed for the solution of equilibrium equations of structures. However, the conventional methods use for structural analysis of nonlinear structures overestimates the displacements when the structures is stiffening and underestimate when it is softening (Ha, 2005). For the conventional method, the number of iteration increases with increase in degree of freedom and these methods need large computer storage for solution of equation of motion. The cable structure is belonged to tension structure.

Equation of motion for a system

The cable structure is multi degree system and the equation of motion for a multi degree system can be written as:

$$M\ddot{X} + C(t)\dot{X} + K(t)X = P(T) \quad (1)$$

Where M= mass matrix; *C (t)* = Damping matrix; *K (t)* = Stiffness matrix; *X* = Displacement vector $\dot{X}$ = Velocity vector; $\ddot{X}$ = Acceleration vector; *P (t)* = Load vector.

Since m is a non-zero constant value, both sides of Equation (1) can be divided by m, and for $P = \frac{C(t)}{M}$ $Q = \frac{K(t)}{M}$ $F = \frac{P(t)}{M}$. Equation 2 can be written as:

$$\ddot{\mathbf{X}} + \mathbf{P}\dot{\mathbf{X}} + \mathbf{QX} = \mathbf{F} \quad (2)$$

The mathematical solution of Equation (2) depends on the values of P, Q and F. Equation (2) is a linear differential equation if P and Q are independent of x and remains so even if P and Q are functions of t.

The method of Fletcher-Reeves

The method avoids explicit construction and inversion of the Hessian matrix k, by using the iterative formula:

$$X_{K+1} = X_k - H_k g_k \quad (3)$$

$$H_k = I + \sum_{i}^{k-1} A_i \quad (4)$$

$$A_i = \frac{V_i V_i^T}{V_i^T x_i} - \frac{H_i \gamma_i \gamma_i^T H_i}{\gamma_i^T H_i \gamma_i} \quad (5)$$

$$\gamma_i = g_{i+1} - g_i \quad (6)$$

In the first iteration H_i = I, the identity matrix. Thus the first step is in the direction of steepest descent. The slow convergency of the steepest descent method is then overcome by choosing the sequence of H such that as i approach k, H_k becomes approximately equal to k^{-1}. For linear problem the method converges in n+1 steps in which case $H_{n+1} = k^{-1}$. It finds the solution to the second equation that is closest to the current estimate and satisfies the curvature condition (Daston, 1979; Farshi and Alinia-Ziazi, 2010). This update maintains the symmetry and positive definiteness of the Hessian matrix. The essential feature of the method is a recursion formula for updating an initial approximation to the Hessian matrix of second partial derivatives of the function to be minimized. The iterative method applied ensures that each step in the procedure leads to a function decrease until a stationary point is reached. The function to be minimized is f(x) where x denotes the argument vector of the decision variables x_1, x_2, ... x_n.

The expression for the total potential energy

The total potential energy is written as:

$$W = U + V \quad (7)$$

Where; W= the total potential energy; U= the strain energy of the system, and V= the potential energy of the loading. Taking the unloaded position of the assembly as datum:

$$W = \sum_{n=1}^{m} U_n + \sum_{j=1}^{j} \sum_{i=1}^{3} F_{ji} X_{ji} \quad (8)$$

Where; M= total number of members; J= total number of cable joints; F_{ji}= external applied load on joint j in direction i, and X_{ji}= displacement of joint j in direction i.

The condition for structural equilibrium is that the total potential energy of the system is a minimum, and is written as:

$$\partial W / \partial X_{ji} = 0 \quad (9)$$

Thus at the solution, the gradient vector of the total potential energy function is zero.

The gradient of the total potential energy

Differentiating Equation (9) with respect to X_{ji} gives the g_{ji} element of the gradient vector g as:

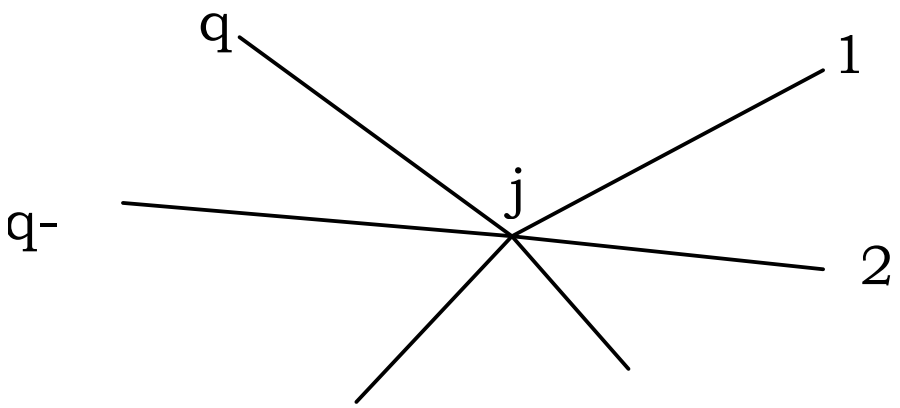

Figure1. General view member's connection.

$$g_{ji} = \partial W / \partial X_{ji} = \sum_{n=1}^{q} \partial U_n / \partial X_{ji} - F_{ji} \quad (10)$$

Let: $T_{\circ jn}$ = the initial tension in member jn; T_{jn} = the instantaneous tension in member jn; e_{jn} = elastic elongation of member jn; E = young Modulus of Elasticity; A = cross-sectional area of cable; L_{jn} = length of member jn and Q = number of member meeting at joint j as shown in Figure 1.

The expression for g_{ji} can then be written as:

$$g_{ji} = \sum_{n=1}^{q} \frac{\partial U_n}{\partial e_{jn}} \cdot \frac{\partial e_{jn}}{\partial X_{ji}} - F_{ji} \quad (11)$$

The strain energy of member j_n is given as:

$$U_{jn} = T_{\circ jn} e_{jn} + \frac{EA}{2L_{jn}} e_{jn}^2 \quad (12)$$

Differentiating U_{jn} with respect to e_{jn} yields:

$$\partial U_{jn} / \partial e_{jn} = T_{\circ jn} + \frac{EA}{L_{jn}} e_{jn} = T_{jn} \quad (13)$$

The initial and elongated length of member j_n may be expressed as:

$$L_{jn}^2 = \sum_{i=1}^{3} (X_{ni} - X_{ji})^2 \quad (14)$$

$$(L_{jn} + e_{jn})^2 = \sum_{i=1}^{3} (X_{ni} - X_{ji} + x_{ni} - x_{ji})^2 \quad (15)$$

Where X_{ji} is the coordinate of joint j in direction i. Simplifying Equation (15) and substituting for L_{jn} from Equation (14) yields the following expression for e_{jn}:

$$e_{jn} = \frac{1}{2L_{jn} + e_{jn}} \sum_{i=1}^{3} \{(X_{ni} - X_{ji}) (2X_{ni} - 2X_{ji} + X_{ni} - X_{ji})\} \quad (16)$$

Differentiating Equation (10) with respect to X_{ji} yields:

$$\partial e_{jn} / \partial X_{ji} = \frac{-1}{L_{jn} + e_{jn}} (X_{ni} - X_{ji} + X_{ni} - X_{ji}) \quad (17)$$

Substituting Equations.10 and17 into Equation (18) yields the expression for the gradient as:

$$g_{ji} = -\sum_{n=1}^{q} t_{jn} (X_{ni} - X_{ji} + X_{ni} - X_{ji}) - F_{ji} \quad (18)$$

Where $t_{jn} = T_{jn} / (L_{jn} + e_{jn})$ is the tension coefficient of member j_n.

Total potential energy in the direction of descent

The correct value of X for which W is a minimum can be found by the iterative process:

$$X_{ji(k+1)} = X_{ji(k)} + S_{(k)} V_{ji(k)} \quad (19)$$

Where the suffices (k) and (k+1) denote the (k)th and (k+1)th iterate respectively and where; V_{ji} = the element of the direction vector, and $S_{(k)}$ = the step length which defines the position along $V_{ji(k)}$ where the total potential energy is a minimum. The

expression for V_{ji} is, if the Fletcher-Reeves formulation method is used (Fletcher, 2007) given by:

$$V_{ji(k)} = -g_{ji(k)} + \frac{\sum_{j=1}^{J}\sum_{i=1}^{3} g_{ji(k)} g_{ji(k)}}{\sum_{j=1}^{J}\sum_{i=1}^{3} g_{ji(k-1)} g_{ji(k-1)}} V_{ji(k-1)} \quad (20)$$

The stationary point in the direction of descent can be found by expressing the total potential energy as a function of the step length along V_{ji} . Thus the required value of $S_{(k)}$ can be determined by the condition and is given (Gloeckner et al., 1976):

$$\partial W_{(k)} / \partial S_{(k)} = 0 \quad (21)$$

Calculation of the step length

The required polynomial for step length is found by substituting the expression for $X_{ji(k+1)}$ given by Equation (19) into a suitable expression for the total potential energy w. Writing the strain energy term in Equation (16) as a function of the elongation, Equation (21), and at the same time substituting for X_{ji} using Equation (19) leads to first the expression for the elongation as a function of S is given as (Kirsch and Bogomolni, 2007):

$$e_{jn} = \frac{1}{2L_{jn} + e_{jn}}(a_1 + a_2 S + a_3 S^2) \quad (22)$$

$$a_1 = \sum_{i=1}^{3}(2(x_{ni} - x_{ji})(x_{ni} - x_{ji}) + (x_{ni} - x_{ji})(x_{ni} - x_{ji}))$$

$$a_2 = \sum_{i=1}^{3} 2((x_{ni} - x_{ji} + x_{ni} - x_{ji})(v_{ni} - v_{ji}))$$

$$a_3 = \sum_{i=1}^{3}(v_{ni} - v_{ji})^2$$

And secondly to the expression for W in terms of the step length S and its derivative with respect to S is given as:

$$W = C_1 S^4 + C_2 S^3 + C_3 S^2 + C_4 S + C_5 \quad (23)$$

$$\partial W / \partial S = 4C_1 S^3 + 3C_2 S^2 + 2C_3 S + C_4 \quad (24)$$

Where;

$$C_1 = \sum_{n=1}^{m}(\frac{EA}{2L(2L+e)^2} a_3^2)_n$$

$$C_2 = \sum_{n=1}^{m}(\frac{EA}{L(2L+e)^2} a_2 a_3)_n$$

$$C_3 = \sum_{n=1}^{m}(\frac{T_\circ}{2L+e} a_3 + \frac{EA}{2L(2L+e)^2}(a_2^2 + 2a_1 a_3))_n$$

$$C_4 = \sum_{n=1}^{m}(\frac{T_\circ}{2L+e} a_2 + \frac{EA}{L(2L+e)^2} a_1 a_2)_n - \sum_{j=1}^{J}\sum_{i=1}^{3} F_{ji} V_{ji}$$

$$C_5 = \sum_{n=1}^{m}(\frac{T_\circ}{2L+e} a_1 + \frac{EA}{2L(2L+e)^2} a_1^2)_n - \sum_{j=1}^{J}\sum_{i=1}^{3} F_{ji} X_{ji}$$

Numerical and experimental testing

The analytical method is used to experiment with mathematical model and experimental work.

a)Theoretical

Theoretical analysis (Mathematical modelling)

The theoretical result based on proposed theory is calculated by structural property matrices below for a pin jointed member with three degrees of freedom at each end is given as follows:

The lumped mass matrices for a pin jointed member

$$\frac{\bar{m}\ L}{3} \begin{vmatrix} 1 & 0 & 0 & 0 & 0 & 0 \\ 0 & 1 & 0 & 0 & 0 & 0 \\ 0 & 0 & 1 & 0 & 0 & 0 \\ 0 & 0 & 0 & 1 & 0 & 0 \\ 0 & 0 & 0 & 0 & 1 & 0 \\ 0 & 0 & 0 & 0 & 0 & 1 \end{vmatrix} \quad (25)$$

Where $\bar{m}$ is the mass and L is the length of member.

The orthogonal damping matrices

This damping matrix in which as many modes can be given by:

$$C = M\left(\sum_{n=1}^{N} \frac{2\varepsilon_n \omega_n}{\phi_n^T M \phi_n} \phi_n \phi_n^T\right) M \quad (26)$$

Where; n = the mode number; ϕ_n = the nth mode shape vector, and M = diagonal mass matrix. The stiffness matrix for a pin jointed member:

$$= \frac{EA}{L} \begin{vmatrix} \lambda_1^2 & \lambda_1\lambda_2 & \lambda_1\lambda_3 \\ \lambda_2\lambda_1 & \lambda_2^2 & \lambda_2\lambda_3 \\ \lambda_3\lambda_1 & \lambda_3\lambda_2 & \lambda_3^2 \end{vmatrix} + \frac{T}{L} \begin{vmatrix} 1-\lambda_1^2 & -\lambda_1\lambda_2 & -\lambda_1\lambda_3 \\ -\lambda_2\lambda_1 & 1-\lambda_2^2 & -\lambda_2\lambda_3 \\ -\lambda_3\lambda_1 & -\lambda_3\lambda_2 & 1-\lambda_3^2 \end{vmatrix} \quad (27)$$

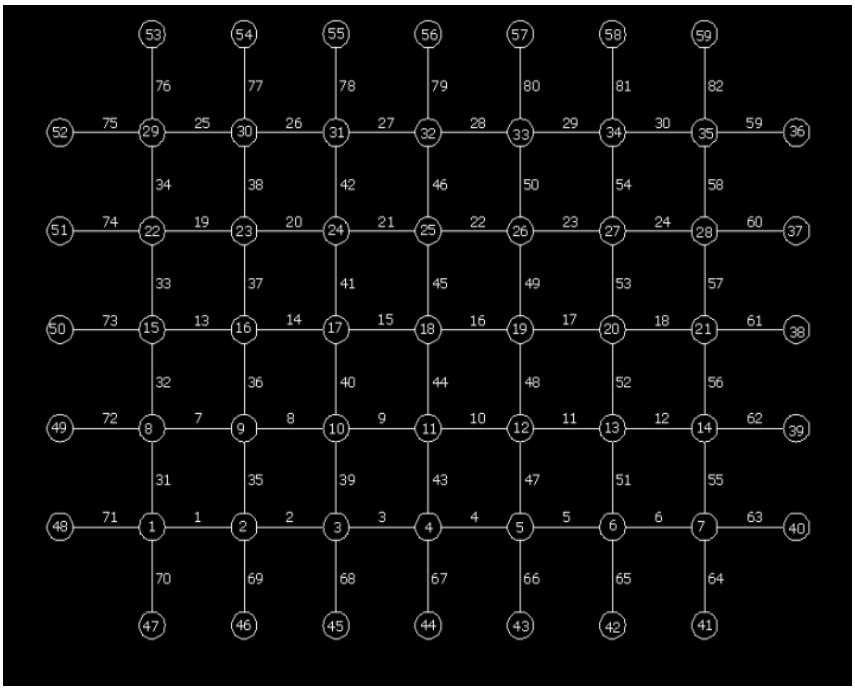

Figure 2. Grid lines of the flat net.

Table Error! No text of specified style in document.**1.** The specifications of flat net and cables.

Description	Details
Overall dimensions	3000*4000
Spacing of the cables	mm
Spacing of the cables	500 mm
Number of free joints	35
Number of fixed joints	24
Number of links	82
Diameter (mm)	15.34
Section Area (mm^2)	142.90
Y/Strength 1% (kN)	244.40
Young's Modulus	192.60 KN/ mm^2
Y/Strength	244.40 KN
Pretension	11500 N/link

Where T is the axial force in the axial force and λ_1, λ_2 and λ_3 are the corresponding direction cosines.

b) Experimental work

The mathematical model chosen is a 7*5 flat net with 105 degrees of freedom. The 7*5 net was built as an experimental model and tested in order to verify the static and dynamic nonlinear Fletcher-Reeves theory. The construction of the experimental model is shown in Figure 2.

The specifications of erected rectangular net and cables are given in Table 1. Each steel cable was initially tensioned to about 1 KN and then left for two weeks to permit the individual wires in the strands to bed in. Then, the tensions on the cables were readjusted to 11.5 KN. This tension was maintained throughout the test programme by checking at interval times. The wedge and barrel used on hollow cylindrical steel to provide endcaster degree of freedom for boundary condition of cables. Endcaster joints are used to fix boundary condition. General view of steel frame is shown in Figure 3, 4 and 5. Specifications of steel frame made are given in Table 2.

The material is homogeneous and isotropic. The stress–strain relationship of all material remains within the linear elastic range during the whole nonlinear response. The external loads are

Figure 3. Construction of frame steel.

Table 2. Features of steel frame made.

Frame supported specification					
Column		**Beam**		**Beam Size**	**Column Size**
1400 mm (box)	Height	300mm * 400mm (box)	Length	100*200*9 mm (hollow section)	200*200*9 mm (hollow section)

displacement independent.

RESULTS AND DISCUSSION

Finite element analysis

The finite element method is a numerical technique for finding approximate solutions of partial differential equations. The finite element analysis uses a complex system of points called nodes which make a grid called a mesh (Sorenson, 1969). This mesh is programmed to contain the material and structural properties which define how the structure will react to certain loading conditions. Nodes are assigned at a certain density throughout the material depending on the anticipated stress levels of a particular area. In this case, the B31 is type of element is used and the details are given in Table 5. In the present study, the modeling space is 3D and wire is used for shape of model. Type of model is deformable and planar. Mass density according libratory testing is 7860 kg/m^3 and Young's Modulus 1.926 N/m^2. Isotropic elastic is type of selected property. Kind of analysis has different steps. The model is considerate symmetric and linear perturbation. General static is selected to analyzing of model. Total number of mesh nodes and mesh linear line elements are 17319 and 17460 respectively type of linear element type is B31 and total number of element 17460.

Static test

Any deficiency in the model could influence the dynamic behavior and make subsequent comparison of experimental and theoretical values difficult. Hence, a Static test is carried out to investigate the degree of symmetric behavior on the frame. The investigation consisted of checking the degree of symmetric behavior about the major and minor axes. The degree of symmetric behavior about the minor axis is investigated by first placing an increasing load on joint 11 and then compares the resultant displacement with those obtained by placing similar loads on joint 25. The degree of symmetric behavior about the major axis is similarly studied by loading first joint 16 and then 20. Figure 5 shows the relationship between loads and deflection in major axis.

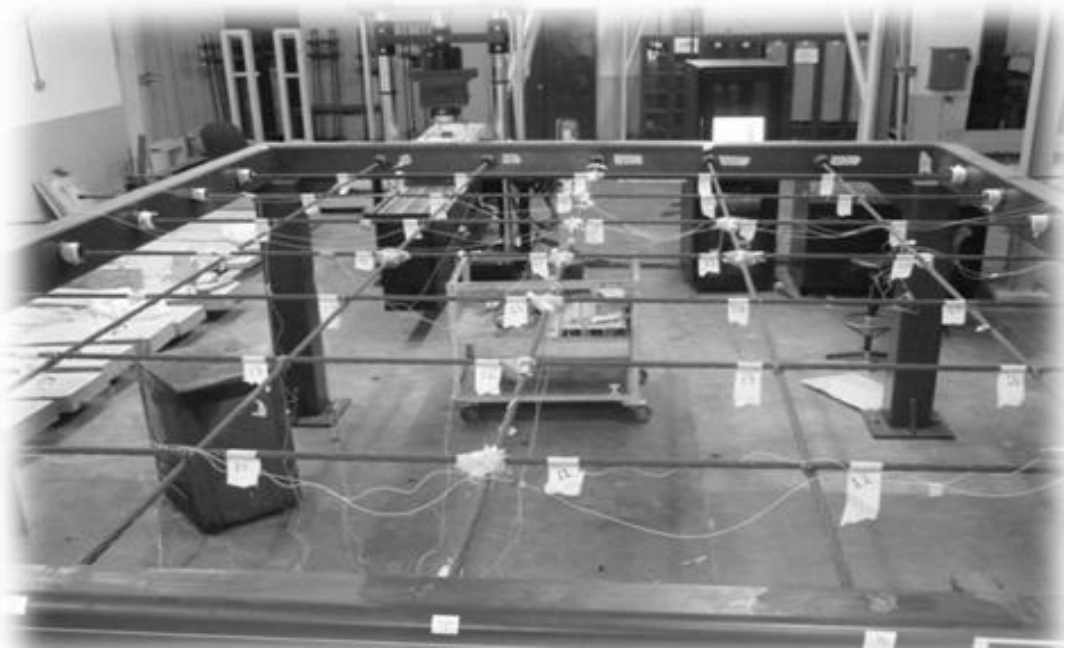

Figure 4. General view of steel frame.

Figure 5. Linear variable differential transformer used on steel frame.

When the concentrated load is placed on node 20, the deflection gradually increased from 0.535 mm on node 15 it reached a peak of 12.7 mm on node 20. From this point onwards, it is projected to drop sharply until it reached 0.607 mm on the node 15. When concentrated load is placed on node 16, the deflection from about 0.607 mm on node 15 rapidly rose to reach a peak of 12.7 mm on node 16. From this point onwards, it is project to fell

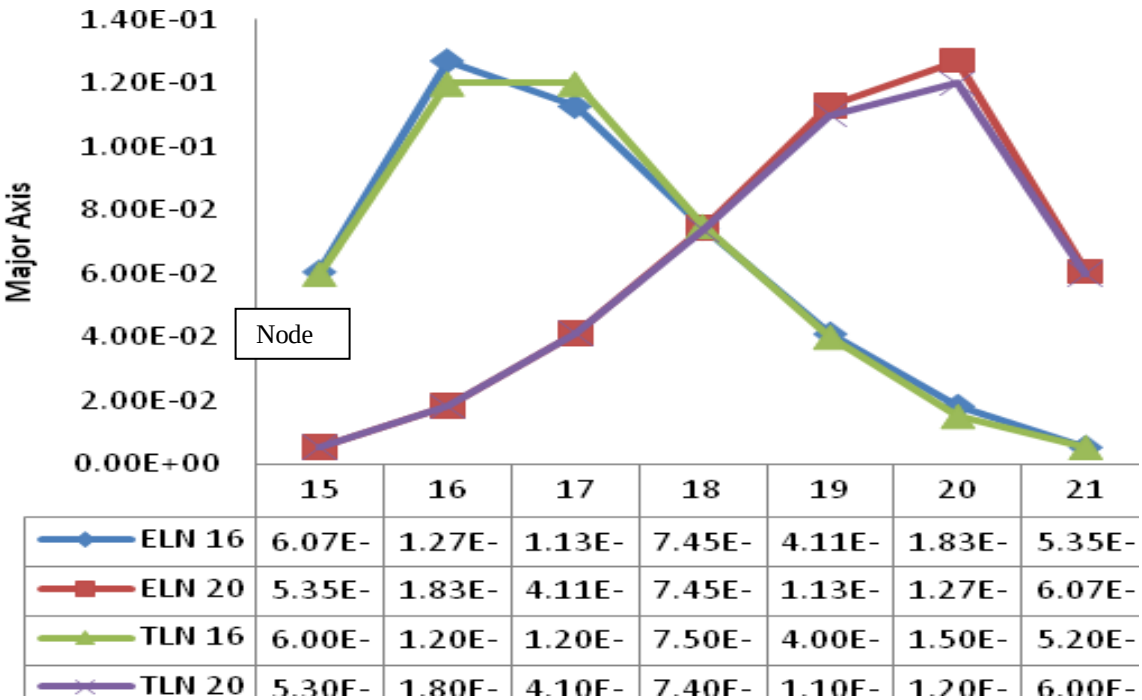

Figure 6. Degree of symmetric about major axis when the load is placed on node 16 and 20. ELN 16, 20: Experimental result of load on nodes 16, 20; TLN 16, 20: Theoretical result of load on nodes 16, 20.

Table 3. Degree of symmetry about the major, minor axes Joint 11, deflections due to concentrated load on joint 11.

Load (N) = 2400	Theoretical (T) Z axis (m)	Experimental (E) Z axis (m)	(T – E) / T*100
Deflections node 18	127.9E-03	125.2E-03	2.11
Deflections node 11	142.3E-03	141.5E-03	0.56
Deflections node 4	67.78E-03	65.28E-03	3.69
Deflections node 25	78.68E-03	77.28E-03	1.78
Deflections node 32	29.54E-0	29.24E-0	1.02
Deflections node 15	20.70E-03	20.32E-03	1.84
Deflections node 16	54.46E-03	53.23E-03	2.26
Deflections node 17	104.2E-03	101.5E-03	2.59
Deflections node 19	104.2E-03	102.1E-03	2.02

slightly until it reached 0.535 mm units on node 21. Degree of symmetry about the major, minor axes Joint 11, deflections due to concentrated load on joint 11 is given in Table 3.

The values between the calculated and measured static deflections are in the same value to each other. A static test checked the stiffness of the boundary and then shows the degree of error for any elastic deformation of the frame is zero. The result verifies the frame is symmetric. Test with different pattern and intensities of static loading in order to compare the experimental and theoretical values of the static deformation showed that the deflection calculated by the proposed nonlinear method gives reasonably accurate results.

Modal test

The objectives of the modal testing described are to verify the dynamic proposed theory. Modal analysis defined as the process of characterizing the dynamics of a structure in terms of its modes of vibration. It turns out that the eigenvalues and eigenvectors which define the resonant frequencies and mode shapes of the modes of vibration of the structure. The time signal graph and excitation force graph for nodes 9 to 16 based on references 3 are shown in Figure 6. The graph of

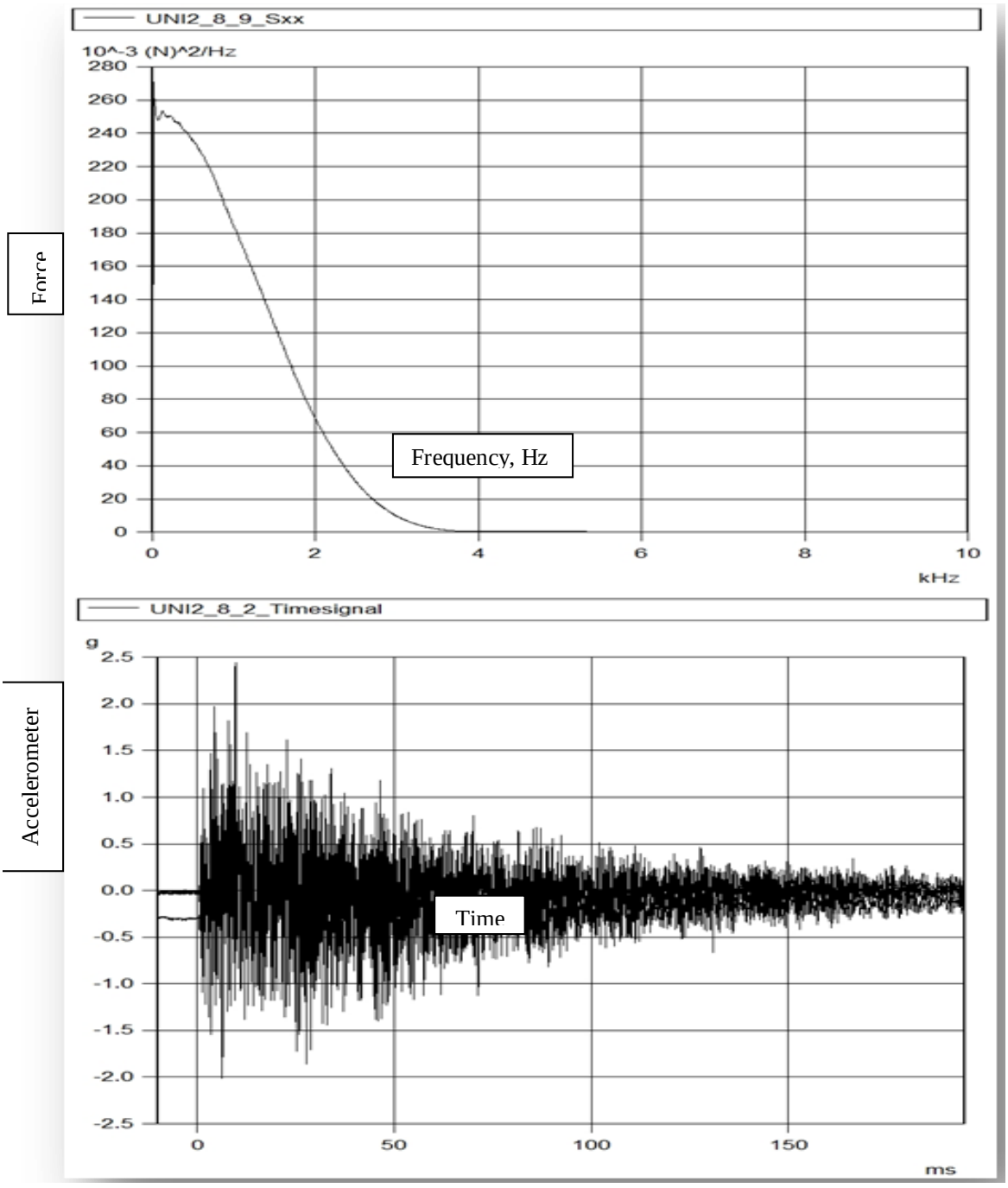

Figure 7. Time signal graph of channel 3 based on reference 3.

excitation for nodes 9 to 16 is shown in Figure 15 and the amplitude of force dropped sharply between 0 and 4 kHz from 270e-3 (N^2/Hz) to 0 units. The time signal bar plot of nodes 9 to 16 in period of 150 milliseconds are also shown in Figure 6F and this figure shows that amplitude of signal for node 10 is highest between 9 and 16 nodes. Table 4 gives the finite element result and theoretical frequencies of net for the five modes. The effect of damping value is calculated by composite modal between mode 1 and mode 5 and load variation with time is detected instantaneous. A result is presented that the natural frequencies decrease only slightly with the increase in the amplitude. It's mean the natural frequency is constant and independent of amount of the force's value. The logarithmic decrement δ against amplitudes of vibration are shown in Figure 8. The logarithmic decrement is calculated from the natural logarithm of the ratio of the amplitudes of any two

Table 4. Theoretical and finite element result of natural frequencies for the five modes.

Load	Natural frequency (Hz) - 0 (N)		
Mode number	Theoretical ω_T	Finite element ω_{FE}	$\frac{\omega_{FE}-\omega_T}{\omega_{FE}}\%$
1	2.9708	2.9531	0.60
2	6.4601	6.4142	0.71
3	8.0102	7.8945	1.44
4	9.1213	9.1023	0.21
5	14.243	14.553	2.18
Load	**Natural frequency (Hz) - 1000 (N)**		
1	2.9708	2.9365	0.57
2	6.4601	6.2356	2.86
3	8.0102	7.6981	2.55
4	9.1213	9.236	1.45
5	14.243	14.6322	0.54

Table 5. Theoretical and finite element result of natural frequencies for the five modes.

Natural frequencies		
ω_T Theoretical	ω_E Experimental	$\frac{\omega_E-\omega_T}{\omega_E}\%$
2.9708	2.9531	0.60
6.4601	6.4142	0.71
8.0102	7.8945	1.44
9.1213	9.1023	0.21
14.243	14.553	2.18

oscillations. Its formulation is:

$$\text{Delta } (\nabla) = \frac{1}{n} \text{Ln } (A_{i+n} / A_i) \quad (28)$$

Where; Ai = amplitude of the ith oscillation; A (i+n) = amplitude of the oscillation n vibrations after the ith oscillation.

By calculating values of δ along the decay curve it was found that the logarithmic decrements varied with the amplitude and reduces with increasing amplitude. During calculation, it appeared that the logarithmic decrement appears to approach a constant value as the amplitude increases. In present work, the free vibration displacement amplitude history of a system to an impulse is calculated and recorded. The logarithmic decrement is the natural logarithmic value of the ratio of two adjacent peak values of displacement in free decay vibration. The comparisons between theoretical and finite element frequencies are in good agreement. As Figures 10 to 14, whole theoretical and experimental mode shapes are close to each other and verify the proposed theory. The modal damping was found by calculating the logarithmic decrement from the decay function. It should mention that logarithmic decrement method is utilized to calculate damping in time domain.

The resulting relationship between degrees of freedom and computing time for 350 iterations for the Fletcher-Reeves and the Newton-Raphson algorithms are shown in Figure 9. Figure shows the computing time against the degree of freedom for Newton Raphson increase sharply but in Fletcher Reeves methods computing time increase slightly. It does seem that the Fletcher-Reeves method result's is sufficient and reasonable for high nonlinearity structures. Hence, the Newton Raphson which is commonly used for system with high degree of freedom cannot achieve accurate result. From the comparisons given in previous Figures and Tables it can be concluded that, the Fletcher-Reeves algorithm is more efficient of

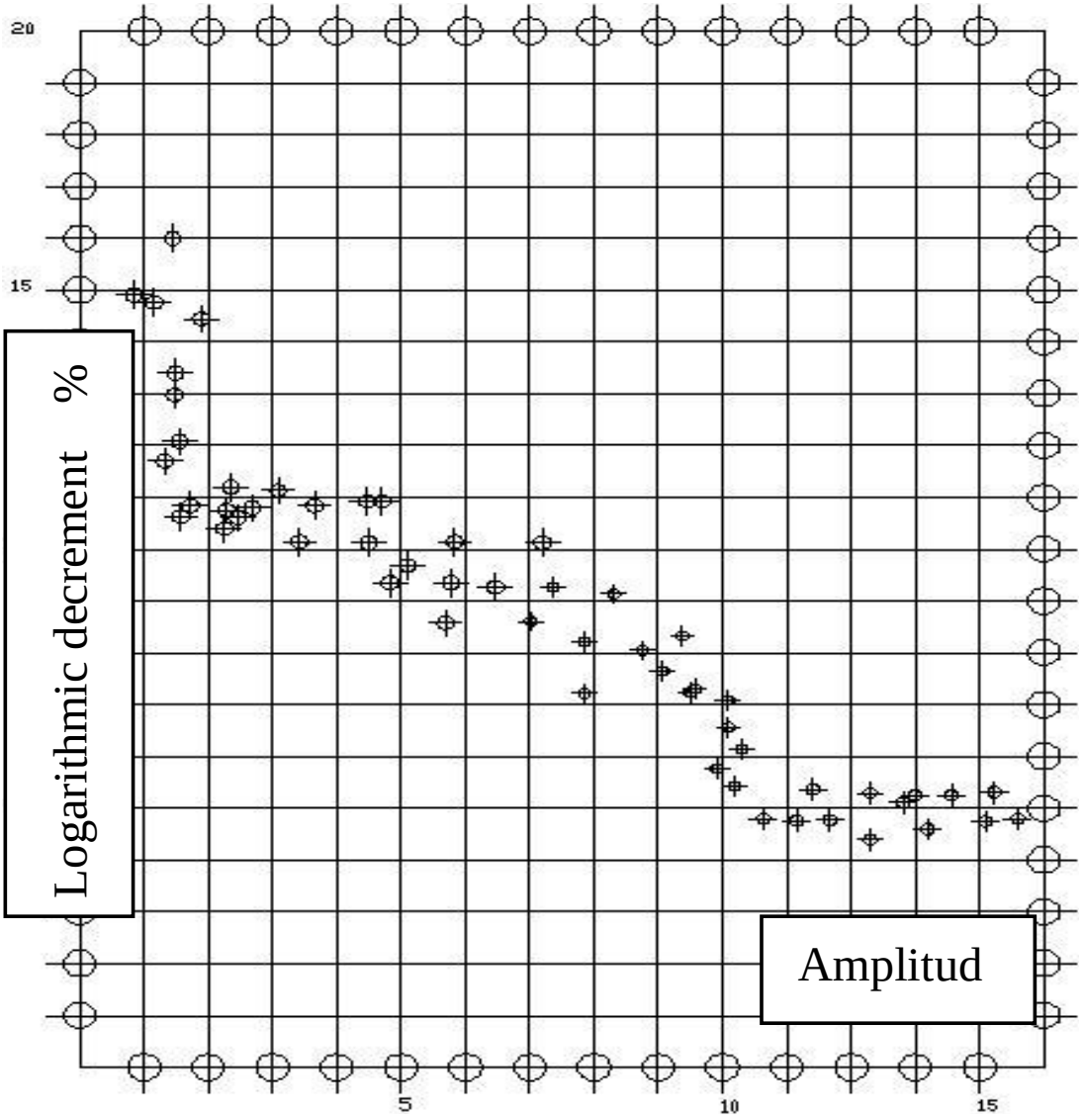

Figure 8. The logarithmic decrements against amplitudes of vibration.

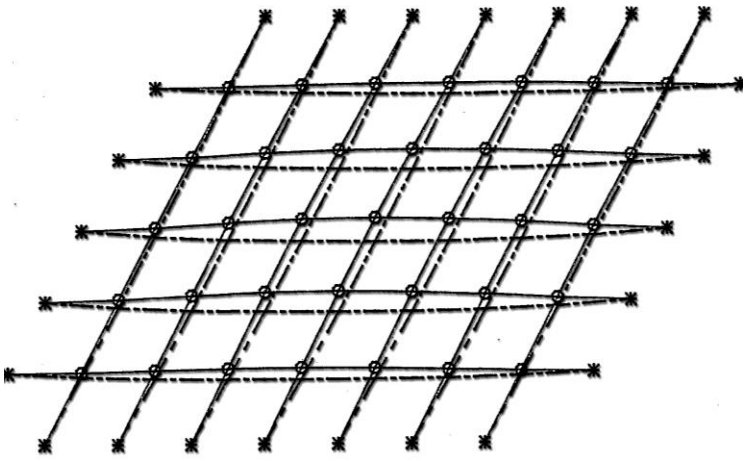

Figure 9. Mode shape 1 of the structure (Theoretical).

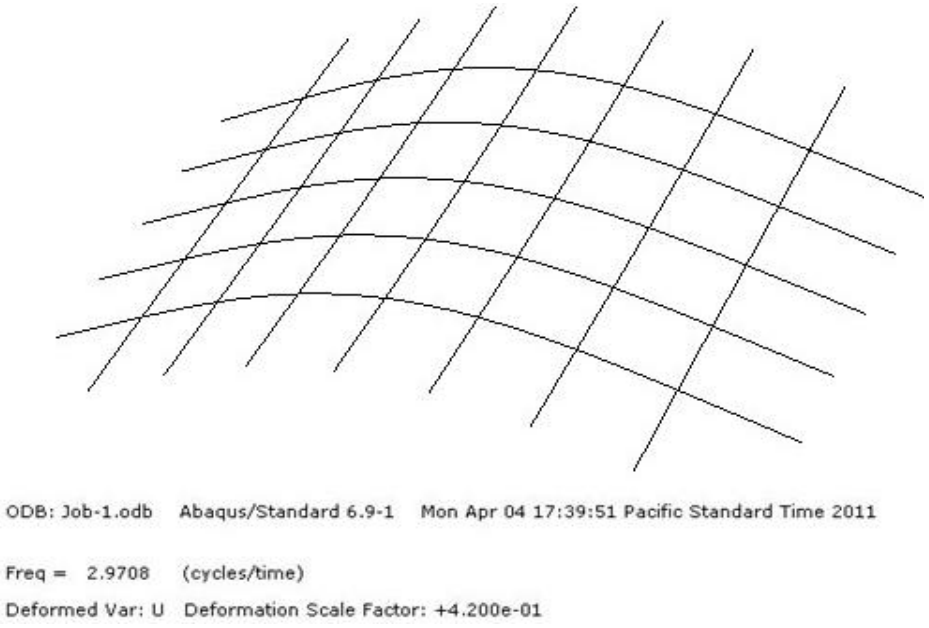

Figure 10. Mode shape 1 of the structure (Finite Element).

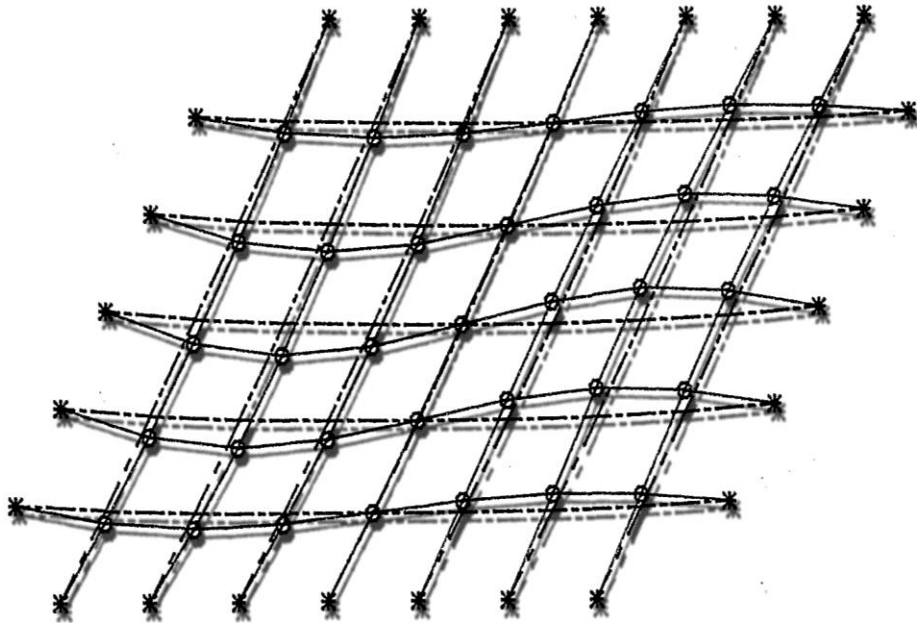

Figure 11. Mode shape 2 of the structure (Theoretical).

the two algorithms used in terms of computing time and storage since both algorithms give almost identical responses.

Conclusions

The values between the calculated and measured static deflections are in good agreement. The comparison of experimental and theoretically predicted values of dynamic response shows that the response calculated by the proposed nonlinear method gives reasonably accurate results. The proposed method was found to be stable for time steps equal to or less than half the smallest time period of the system. The experimental work carried out by static and dynamic testing of the flat

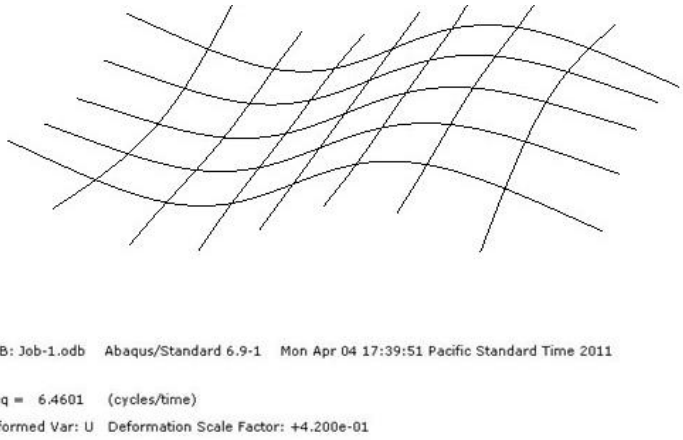

Figure 12. Mode shape 2 of the structure (Finite Element).

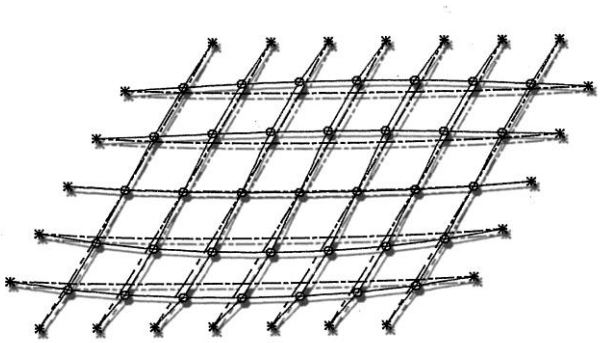

Figure 13. Mode shape 3 of the structure (Theoretical).

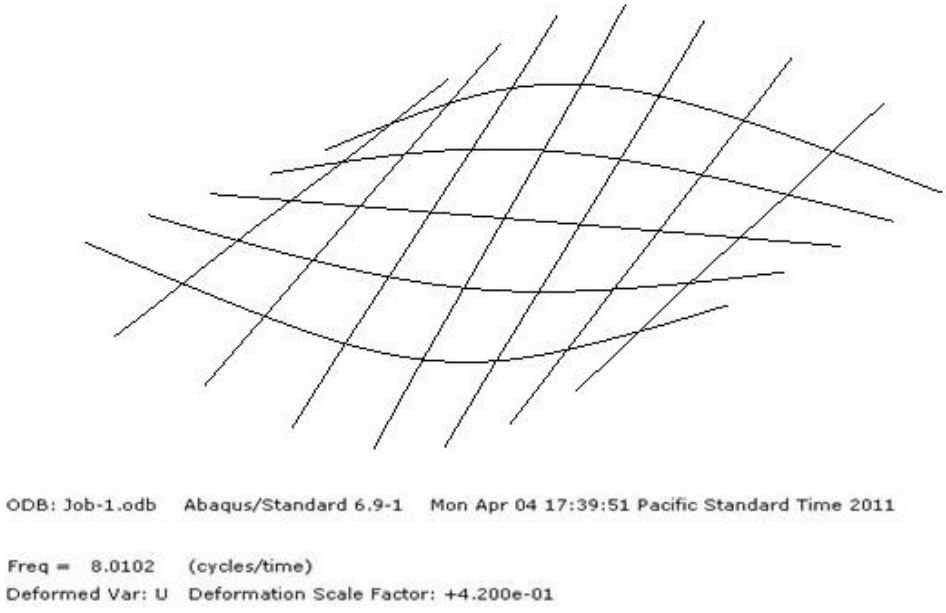

Figure 14. Mode shape 3 of the structure (Finite Element).

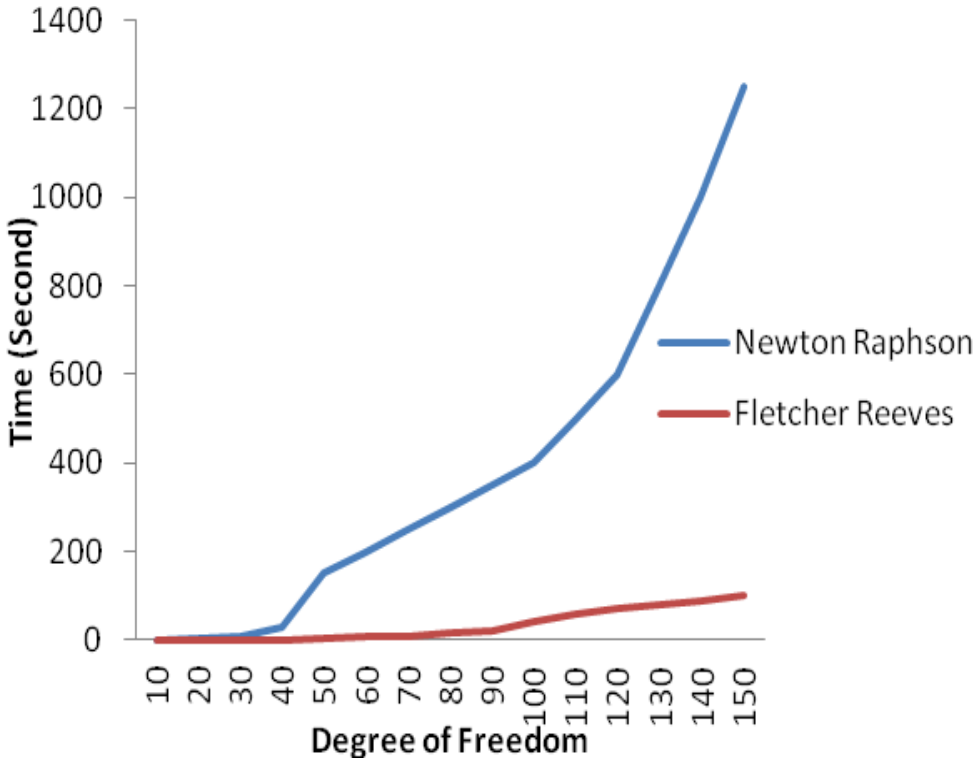

Figure 15. Visual relationship between degrees of freedom and computing time.

net showed good agreement between the experimental result and theoretically predicted values. The percentage differences between the theoretical and experimental results did not in any case exceed 10%. This is thought to be acceptable.

Finally, it be concluded that, the Fletcher-Reeves algorithm is more efficient in terms of computing time and storage practically in high nonlinear structures.

REFERENCES

Aschheim M, Tjhin T, Comartin C, Hamburger R, Inel M (2007). The scaled nonlinear dynamic procedure. *Eng. Struct.,* 29(7): 1422-1441.

Buchholdt HA, Moossavinejad S (1982). Nonlinear dynamic response analysis using conjugate gradients. *Eng. Struct.,* 4(1): 44-52.

Daston LJ (1979). D'Alembert's critique of probability theory. Historia Mathematica, 6(3): 259-279.

Fletcher R (2007). Methods for the solution of optimization problems. Comput. Phys. Commun., 3(3): 159-172.

Farshi B, Alinia-Ziazi A (2010). Sizing optimization of truss structures by method of centers and force formulation. Int. J. Solids Struct., 47(18-19): 2508-2524.

Gloeckner DH, Macfarlane MH, Pieper SC (1976). The use of first and second derivatives in optical model parameter searches. Comput. Phys. Commun., 11(3): 299-312.

Ha TXD (2005). Lagrange multipliers for set-valued optimization problems associated with coderivatives. J. Math. Anal. Appl., 311(2): 647-663.

Hashamdar H, Ibrahim Z, Jameel M, Mahmud HB (2011a). Renovation explicit dynamic procedures by application of Trujillo algorithm. Int. J. Phys. Sci., 6(2): 255-266.

Kukreti AR (1989). Dynamic response analysis of nonlinear structural systems subject to component changes. Comput. Struct., 32(1): 201-212.

Kirsch U, Bogomolni M (2007). Nonlinear and dynamic structural analysis using combined approximations. Comput. Struct., 85(10): 566-578.

Sorenson HW (1969). Comparison of some conjugate direction procedures for function minimization. J. Franklin Instit., 288(6): 421-441.